

Optimisation of compaction and liquid-state sintering in sintering and dissolution process for manufacturing Al foams

Yuyuan Zhao^{a,*}, Fusheng Han^{a,b}, Thomas Fung^a

^a Department of Engineering, The University of Liverpool, Liverpool L69 3GH, UK

^b Institute of Solid State Physics, Chinese Academy of Sciences, Hefei 230031, China

Received 19 September 2002; received in revised form 30 July 2003

Abstract

The effects of the compaction and liquid-state sintering conditions on the structure of the resultant Al foams manufactured by the sintering and dissolution process have been studied. The cell morphology and size of the final Al foam closely match those of the NaCl particles used. The foam porosity is 2–4% higher than the initial volume percentage of NaCl in the Al/NaCl powder mixture due to the contributions from green porosity and shrinkage. The microstructure of the Al matrix is characterised by an interconnected metallic framework with the presence of discontinuous interstices and fine voids as well as primitive particle boundaries in the cell walls. The optimum ranges of compaction pressure and sintering temperature are 200–250 MPa and 670–680 °C, respectively. Adding elemental Mg powder in the compacts has little effect on sintering. Adding elemental Sn together with Mg powders creates a densified Al matrix.

© 2003 Elsevier B.V. All rights reserved.

Keywords: Compaction; Liquid-state sintering; Al foam; Sintering; Dissolution process

1. Introduction

Cellular metallic materials have attracted more and more attention in the last few decades with increased availability of practical manufacturing technologies and improved understanding of their physical, chemical and mechanical properties [1,2]. There is a great diversity of cellular metallic materials that show various structures and properties, which has been described in detail by Banhart [2]. According to the connectivity of cells, cellular metals can be categorised as either closed- or open-celled. Like natural cellular materials, cellular metals are also dominantly used for light-weight constructional or functional purposes. In most cases, the functions such as filtration, separation, heat or mass exchange, and sound or energy absorption require open-celled structures. Therefore, cellular metallic materials with open-celled structures have wider applications in functional structures.

There are a variety of ways to produce open-celled cellular metals, in which liquid infiltration (including both invest-

ment casting and preform infiltration) and electro-deposition techniques are the most widely used routes. Only the former is applicable for aluminium alloys whereas the latter are mainly used for nickel or nickel–chromium alloys [2]. There are still some restrictions to the structures obtainable by the liquid infiltration technology, since the structure parameters like cell size, cell shape and porosity are determined to a large extent by the precursor filler materials. For example, the porosity is usually lower than 70% and cell sizes larger than 0.5 mm in preform infiltration [3], while investment casting allows producing Al foams with higher porosities (>80%) and larger cell sizes (>0.8 mm) [2]. These restrictions in structures can result in a limited range of properties and thus less broad applications. It is therefore necessary to develop more flexible technologies to offer a wider range of structures and properties.

Zhao and Sun [4] have recently developed a promising alternative for manufacturing open-celled Al foams via the conventional powder metallurgy (P/M) route, known as the sintering and dissolution process (SDP). This approach consists of three stages. Firstly, a mixture of Al and NaCl powders is die-pressed into a green compact under an appropriate pressure. Secondly, the compact is sintered at a temperature either above or below the melting point of Al

* Corresponding author. Tel.: +44-151-794-46-97; fax: +44-151-794-46-75.

E-mail address: y.y.zhao@liv.ac.uk (Y. Zhao).

to form a well-bonded and net-shaped structure. Finally, the NaCl particles are removed by leaching the sintered compact in hot water, leaving behind an open-celled Al foam. In comparison to the liquid preform infiltration process, the most outstanding technical advantages of SDP arise from the much wider achievable ranges of structure parameters. In the liquid infiltration process, the porosity of the as-manufactured foam is determined by the density of the pre-prepared compact of the NaCl powder. Because the density of the compact falls within a relatively narrow range between the apparent density and the tap density of the powder, the porosity of the resultant foam is more or less fixed. It is also difficult to reduce the cell sizes of the foam to below 0.5 mm, although in theory smaller cell sizes can be obtained by using a NaCl powder with the particles finer than 0.5 mm. This is because the greatly reduced interstices in a compact of very fine NaCl particles inhibit the full infiltration by the Al melt due to the fact that liquid Al does not wet NaCl. In SDP the foam porosity can be varied in a much wider range by adjusting the NaCl-to-Al volume ratio in the NaCl/Al powder compact, as long as both the NaCl particles and the Al matrix are interconnected in the great majority. SDP can use finer NaCl particles to produce fine-celled foams because the interstices between the NaCl particles are filled with Al particles in the solid state. Consequently, the Al foams produced by SDP are expected to be able to meet the property requirements in a wide range of applications. However, the sintering mechanism and associated phenomena in SDP are still not fully understood due to the particularity of Al powder. The dependence of the final structure on the processing conditions, particularly in the compaction and sintering stages, and materials parameters also needs to be further investigated.

Powder sintering technologies can be roughly divided into two main forms in terms of whether a liquid phase is present or not, i.e. solid-state sintering or liquid-phase sintering. Solid-state sintering may not be the best solution for Al powder sintering due to the following reasons. It is commonly recognised that it is difficult to establish a metallurgical bonding in a packed Al powder during sintering at a temperature below its melting point, because the Al particles are usually covered by a thermochemically stable Al_2O_3 film [5]. This prevents mass transport by diffusion, because of the extremely low-reactive diffusion rates in this dense and stable oxide layer. To circumvent this problem, measures must be taken to eliminate the oxide film and to create metallic contacts between the Al particles. There are two approaches that may attain this. One is deforming the powder mixture to break up the oxide film. Efficient rupture of the oxide film can be achieved by applying a high compaction pressure and more effectively by adding rigid ceramic particulates to the mixture [6,7]. The other is employing highly reactive elements such as Mg, either alloyed in the Al powder beforehand, or added in the powder mixture in the form of an elemental powder [5–9]. Mg acts as a solid reducing agent in the system because the free energies of formation

of the resultant Mg oxides, MgAl_2O_4 and MgO, are lower than that of Al_2O_3 . Al foams have successfully been made by SDP via solid-state sintering by combining high compaction pressure and Mg addition [10]. However, solid-state sintering of Al/NaCl compact is a very time-consuming process and may not be practical for large-scale commercial applications.

It has long been known that the formation of a liquid phase during sintering can significantly accelerate mass transport [11–15]. Liquid-phase sintering has become a more universally applied process and over 70% of sintered products in the P/M industry are manufactured by this route [13]. This route is more appropriate than solid-state sintering for oxide-covered particles such as Al. It should, however, be noted that the liquid phase formed (usually an eutectic) must highly wet the solid phase for effective sintering. Additionally, it has been reported that Sn is an ideal sintering aid for the sintering of Al and the effectiveness can be noticeably enhanced in the presence of Mg [5].

A higher pressure is generally desirable when compacting a powder sample in the P/M practice, regardless of the sintering technologies employed. The higher the compaction pressure, the higher the sintering rate and the final density, because of reduced green porosity and increased dislocation population. However, excessively high pressure should be avoided because it is neither practical for intended applications nor beneficial to the final microstructures in most materials [12]. It has been proposed that the maximum relative green density should not exceed 92% [12]. In SDP, it is more complicated because the powder mixture contains a high proportion of NaCl particles. The brittle NaCl particles are liable to be crushed if too high a pressure is applied. There likely exists an optimum range of compacting pressure.

The present study aims to study the relationship between the processing conditions and the microstructure of the resultant foam and also to optimise the most important parameters in the compaction and sintering stages in SDP, i.e. compaction pressure and sintering temperature.

2. Experimental

The raw materials are mainly atomised elemental Al powder and culinary NaCl powder. Elemental Sn and Mg powders with a similar particle size to the Al powder were added in some compacts in order to investigate their effects on sintering in the present conditions. The typical morphologies of the Al and NaCl powders are shown in Fig. 1. The majority of the Al particles are rounded but irregular-shaped with a mean diameter of $\sim 50 \mu\text{m}$ and an aspect ratio of ~ 2 . The NaCl particles are roughly cubic with rounded edges. In order to control the cell sizes of the final foam to within a relatively small range, the NaCl powder was divided by a series of sieves into four size groups: 250–425, 425–710, 710–1000 and 1000–2000 μm , with nominal mean sizes of 338, 568, 855 and 1500 μm , respectively.

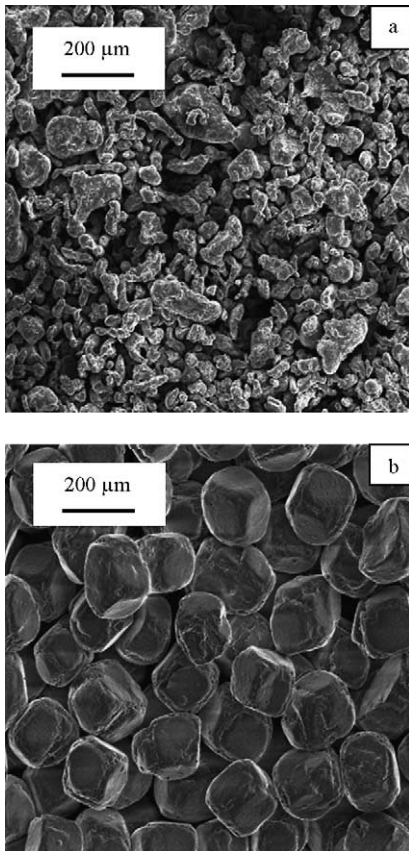


Fig. 1. Typical morphologies of raw powders: (a) Al and (b) NaCl.

In the preparation of each green compact, the Al powder and the NaCl powder with a chosen particle size range (and the Sn and Mg powders wherever appropriate) were weighed using an electronic balance with an accuracy of 0.01 g. The weights were converted into volumes and thus the volume fraction of NaCl in the powder mixture was obtained. The volume fraction of NaCl was varied from 60 to 80%. The powders were then mechanically blended until full homogeneity was achieved. A small amount of water (~1%) was sprinkled during blending to prevent the dissimilar powders from segregation. The mixture was uniaxially pressed at a given pressure, varied over a range of 100–350 MPa, in a stainless steel tube with an i.d. of 35 mm and a height of 80 mm. The compact contained in the tube was heated at 150 °C for 30 min to remove both absorbed and crystalline water in the NaCl particles and any residual water in the compact. The two bare surfaces of the compact were then sealed with water-glass to separate it from the air atmosphere. The sintering of the compact was performed in a resistance furnace. The sintering temperatures varied between 665 and 685 °C at intervals of 5 °C while the holding times were fixed at 3 h. After sintering was completed, the compact-tube assembly was removed from the furnace and allowed to cool naturally to room temperature. The sintered compact was then slowly pushed out of the tube, followed by grinding or machining to the required geometry. Finally,

the imbedded NaCl particles were leached out by placing the sintered compact in hot water at ~95 °C for ~4 h, leaving behind a highly porous metallic framework.

The porosity of the green Al/NaCl compact, P_c , can be estimated by the simple equation

$$P_c = \frac{1 - \rho_c}{\rho_s} \quad (1)$$

where ρ_c is the density of the green compact and ρ_s is the theoretical density of a fully dense Al/NaCl mixture with the same NaCl/Al ratio as the compact. The density of the compact, ρ_c , was determined by measuring its dimensions and mass whereas the theoretical density of the dense mixture, ρ_s , was calculated by the rule of mixtures:

$$\rho_s = \rho_{Al} V_{Al} + \rho_{NaCl} (1 - V_{Al}) \quad (2)$$

where ρ_{Al} and ρ_{NaCl} are the densities of Al and NaCl, respectively, and V_{Al} is the volume fraction of Al in the Al/NaCl mixture. Similarly, the porosity of the as-manufactured Al foam, P_f , can be estimated by

$$P_f = \frac{1 - \rho_f}{\rho_{Al}} \quad (3)$$

where ρ_f is the measured density of the foam.

The structure of the Al foams, including cell morphology and cell wall microstructure, was examined under an optical microscope and a Hitachi S-2460N scanning electron microscope (SEM). For the optical examinations, the pores of the samples were filled with a cold-hardening epoxy resin before grinding and polishing.

3. Results

3.1. Compaction pressure

Fig. 2 shows the porosity and density of the green compacts as a function of compaction pressure, with different NaCl particle sizes, and NaCl/Al volume ratio in the compacts. The green density and porosity seem insensitive to the NaCl particle size as shown in Fig. 2a. They are only dependent on the compaction pressure and the NaCl/Al ratio in the compact. The green porosity decreases linearly with increasing compaction pressure or NaCl/Al ratio.

Fig. 3 shows the defective Al foam samples produced under unsuitable compaction pressures. At a compaction pressure lower than 200 MPa, there was severe spalling of Al particles yielding an imperfect geometry. At a compaction pressure higher than 300 MPa, cracks were often induced in the samples, sometimes leading to complete fracture, although strong bonding was observed in the undamaged regions in the samples. The samples produced under medium compaction pressures in the range 200–250 MPa exhibited the highest qualities, as shown in Fig. 4. These foam samples retained their original shapes, including sharp edges, and had satisfactory strength.

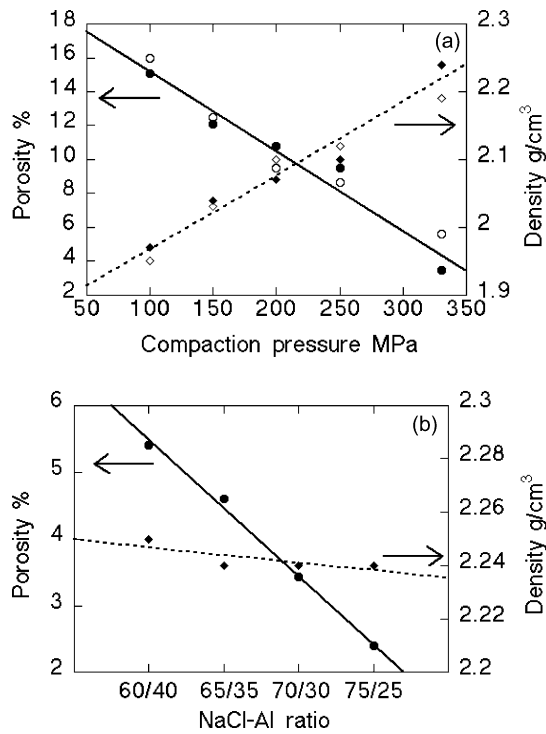


Fig. 2. Variations of porosity and density of green compacts with compaction pressure and NaCl/Al ratio: (a) mean NaCl particle sizes: 338 μm (\bullet , \blacklozenge) and 1500 μm (\circ , \blacklozenge); NaCl/Al ratio: 70:30, and (b) mean NaCl particle size: 338 μm and compaction pressure: 330 MPa.

3.2. Sintering temperature

When the sintering temperature was below 670 $^{\circ}\text{C}$, completely intact Al foam samples could not be produced at the given holding time of 3 h. All the compacts collapsed in the subsequent leaching process. When the sintering temperature was above 680 $^{\circ}\text{C}$, some Al oozed out of the surface of the compacts in the form of globules, although effective bonding was achieved. The size of the Al globules increased with sintering temperature. The loss of Al from the compact led to inhomogeneous cell wall structure and cell size dis-

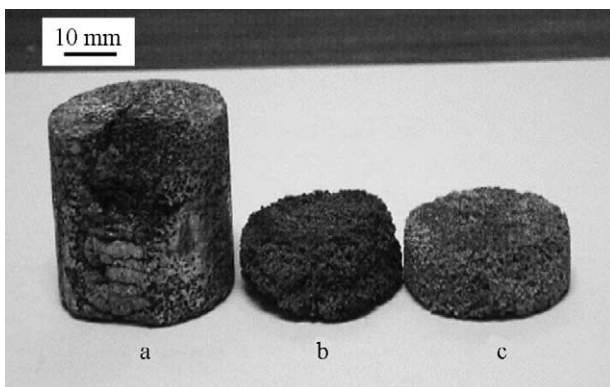


Fig. 3. Typical flaws resulting from unsuitable compaction pressures: (a) cracking and fracture at 300 MPa, (b) severe spalling at 100 MPa and (c) reduced spalling at 150 MPa.

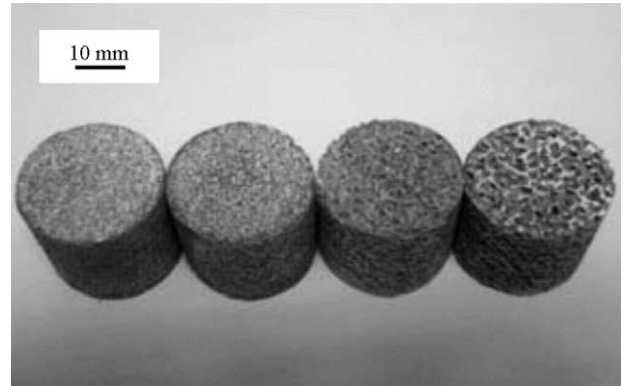


Fig. 4. Examples of Al foam samples manufactured under optimised processing conditions with mean cell sizes of 338, 855, 1500 and 3000 μm (from left to right).

tribution. When the sintering temperature was controlled in the range 670–680 $^{\circ}\text{C}$, the quality of the samples was generally satisfactory. The sintering temperature for the foam samples in the following sections was all fixed at 680 $^{\circ}\text{C}$.

3.3. Porosity of Al foams

Fig. 5 shows a comparison between the final porosity of the Al foam and the initial volume fraction of the NaCl powder in the Al/NaCl powder mixture. The foam porosity is 2–4% higher than the initial volume fraction of NaCl, and the higher the NaCl volume fraction, the lower the increase in foam porosity.

3.4. Structure of Al foams

Fig. 6 shows the typical macroscopic structure of the present Al foams. The porosity of the foams shown in Fig. 6a and b are 83 and 63%, respectively. The particles of the NaCl powders used in producing the foams are roughly cubic with rounded edges and the particle size ranges are: (a) 300–1000 μm [4] and (b) 425–710 μm . It is shown that the cells in the structures are virtually negative replicas of the NaCl particles and the cell sizes match closely with the par-

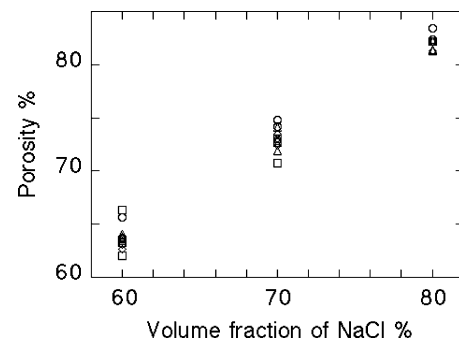


Fig. 5. Relationship between volume percentage of NaCl in green compact and porosity in the final Al foam with mean cell sizes of 338 μm (\diamond), 855 μm (\square), 1500 μm (\triangle) and 3000 μm (\circ).

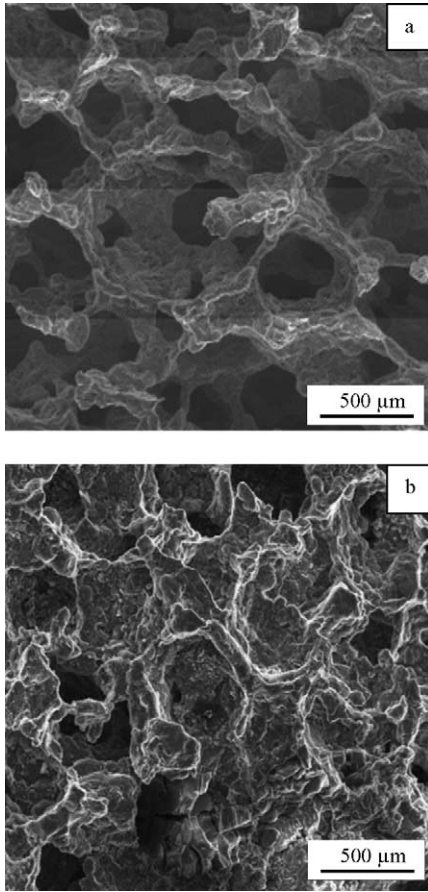


Fig. 6. Typical cell morphologies of Al foams made by SDP with a porosity of (a) 85% [4] and (b) 62%.

ticle sizes. However, the internal surfaces of the cells are rough and do not reflect the surface quality of the NaCl particles on a microscopic level. Fig. 7 shows the typical microstructure of the cell walls. The cell walls are not dense but dispersed with a large number of micro pores or interstices, which form numerous channels between the neighbouring cells. In the dense regions of the cell walls, some boundaries between the original Al particles (deformed during compaction) are still visible. This shows that the oxide layer of the Al particles is not fully broken during compaction and the Al particles are, therefore, not completely fused during sintering.

3.5. Effects of Sn and Mg

Fig. 8 shows the microstructure of the Al foams where small amounts of Sn and Mg, or solely Mg had been added to the powder mixtures as elemental powders before compaction and sintering. As having been shown in Fig. 7a and b, a large quantity of micro pores and interstices exist in the matrix of the pure Al foams. There is very little change in the matrix microstructure for the foam after 0.5 wt.% Mg addition, relative to the Al powder, as shown by comparing

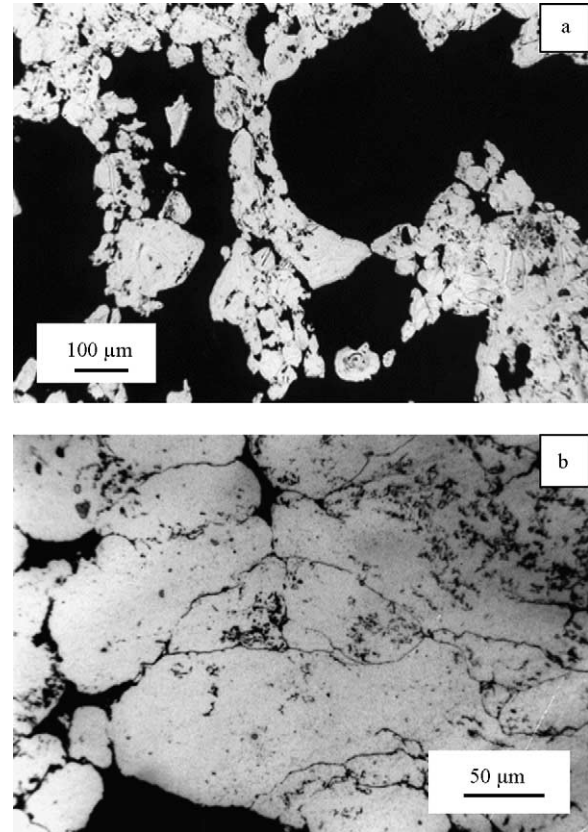


Fig. 7. Typical microstructure of the cell walls in Al foams made by SDP with a magnification of (a) 60 \times and (b) 200 \times .

Fig. 8a and c with Fig. 7a and b. Unlike in solid-state sintering [10], the addition of elemental Mg powder did not seem to introduce a large difference in the liquid-state sintering of Al powder under the present conditions. When both Sn and Mg were added, both at 0.5 wt%, however, the foam exhibited a densified matrix as shown in Fig. 8b and d.

4. Discussion

4.1. Compaction

It is well documented that effective solid-state sintering of Al powder can only be achieved after a considerable amount of the oxide film at the surface of the Al particles is disrupted either by mechanical deformation during compaction or Mg reduction during sintering [5–10]. To achieve strong metallurgical bonding during liquid-state sintering of Al powder, the oxide film at the surface of the Al particles must also be first disrupted, otherwise, the oxide film of each particle will serve as a hard shell preventing the Al inside, even in the liquid form, from establishing direct contact with fresh Al in the adjacent particles.

Mechanical destruction of the oxide film during compaction is an essential measure for promoting the subsequent

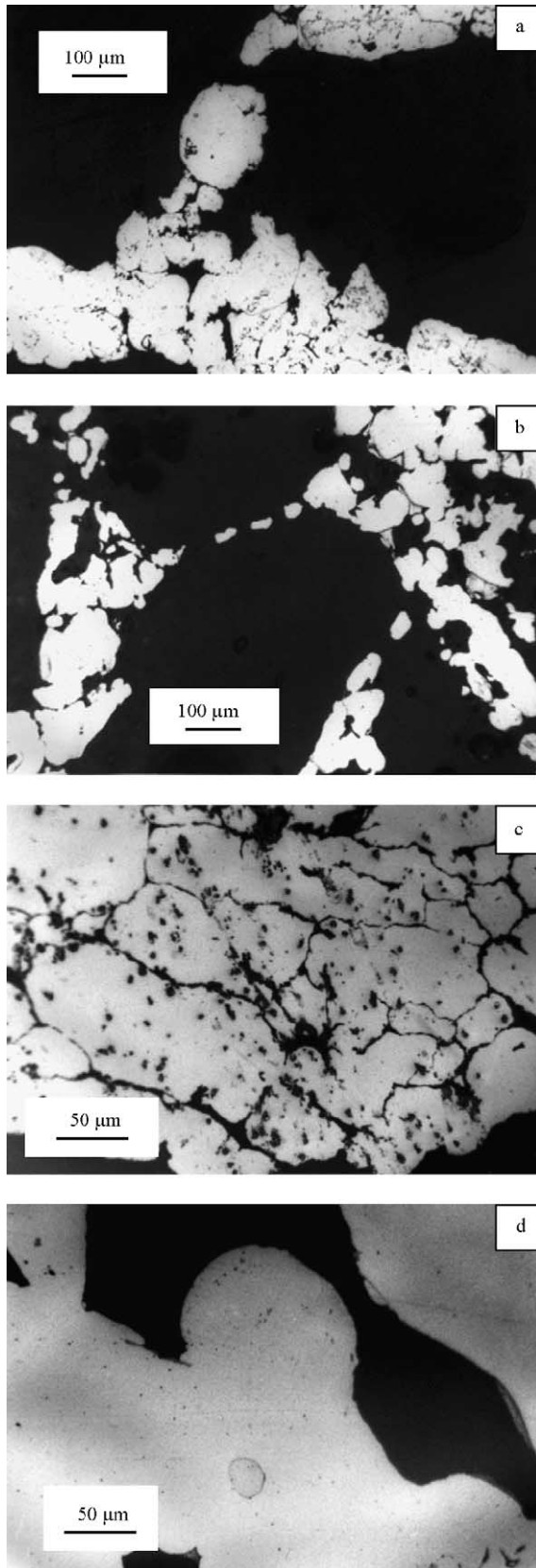


Fig. 8. Effects of Sn and Mg additions on matrix microstructure of Al foams: (a) 0.5 wt.% Mg, (b) 0.5 wt.% Sn + 0.5 wt.% Mg, (c) same as 'a' but locally magnified, and (d) same as 'b' but locally magnified.

sintering. This is realised in SDP by applying a relatively high compaction pressure compared with that in ordinary P/M production. Two mechanisms may take effect in SDP. Firstly, a high pressure yields a large shear strain and stress concentration in the regions of the Al particles in direct contact with the neighbouring particles, which leads to the deformation of the Al particles, the fracture of the oxide films and the formation of fresh metallic contacts. Secondly, the hard NaCl particles can scratch and jab into the Al particles and thus rupture the oxide films during the rearrangement of the particles under a high compaction pressure. The fresh metal–metal contacts formed during compaction are fused together in the subsequent sintering process and become effective bonding points between the Al particles. As a consequence, an interconnected metallic framework is formed as evident in the microstructure of the matrix as shown in Fig. 7.

Fig. 2 shows that the green porosity decreases linearly with increasing compaction pressure or NaCl/Al ratio but is largely independent of the NaCl particle size. This fact suggests that the distribution of strain may be more uniform in a compact containing more rigid particles such that the overall deformation of the much softer Al particles is enhanced. From the process–control point of view, the compaction pressure needs to be adjusted with NaCl/Al ratio in the compact. The compaction pressure corresponding to a relative green density of 92%, which was proposed as the maximum relative green density allowed for metal compacts [12], or a porosity of 8%, is 250 MPa. If the above criterion is also assumed to apply to the Al/NaCl compacts, the compaction pressure should also not be above 250 MPa.

The inspection of the Al foam samples manufactured under different compaction pressures confirms that compaction pressure does have a determinative influence on the bonding between the Al particles formed in the subsequent sintering stage. The optimum compaction pressure lies in the range 200–250 MPa. At lower compaction pressures, intimate fresh metallic contacts between the Al particles are unlikely to be achieved. At higher compaction pressures, the samples often crack during sintering.

The cell walls in the Al foams manufactured under the medium compaction pressures between 200 and 250 MPa, however, are not fully dense but contain some interstices, or voids, which have almost certainly existed in the green compact and are retained after sintering. The primitive particle boundaries can still be discerned in the cell walls, even in the dense regions. The microstructure of the cell walls suggests that a large proportion of the oxide film at the Al particle surfaces is not broken. This may be understood by considering the stress and strain distributions in the Al/NaCl compact during compaction. The Al and NaCl powders used in SDP have different particle morphologies and sizes, as shown in Fig. 1, and more importantly very different mechanical properties. The former is ductile and soft while the latter brittle and hard. The Al particles close to the NaCl particles are usually subjected to higher strains and the oxide films at their surfaces are more likely to be disrupted. Further, from

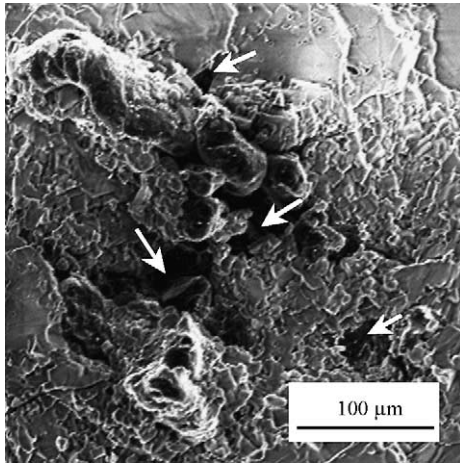


Fig. 9. Microstructure of the Al matrix showing voids between the original Al particles.

the Al/NaCl contacts, the strains are lower and the oxide films are likely to remain intact. In certain extreme conditions, the local Al particles may not undergo much deformation and the destruction of the oxide film may not occur at all. For instance, very little stress and therefore strain may be present in the Al particles surrounded by touching NaCl particles. Fig. 9 shows the microstructure of the Al matrix where several voids are clearly present (see arrows). Very little deformation is observed, because the stress should be the lowest in the regions around the voids. The distributions of stress and strain in the Al/NaCl compact, and thus the fresh metal contacts, are therefore inhomogeneous. Increasing compaction pressure can improve the bonding in the Al matrix because of increased fresh metal contacts between the Al particles. Excessively high compaction pressure is not only difficult to achieve in practice but also likely to bring about undesirable defects in the final Al foam. In addition to the aforementioned cracking and fracture problems, it can also lead to fragmentation of the NaCl particles.

4.2. Sintering

Selection of an appropriate sintering temperature is important. The rapid formation of effective bonding between the Al particles in liquid-state sintering is fulfilled by the localised fusion of the particles provided that the particles are not completely separated by oxide films. As described above, the number of intimate metal–metal contacts is limited compared with the total interfacial area among the Al particles. Minute gaps may also form at the fresh metal contacts as a consequence of stress relief after the compaction operation. It is therefore desirable for the molten Al to have a certain degree of fluidity, i.e. relatively low viscosity, so that the neighbouring particles can be effectively bridged and bonded even if the contacts are not perfect. The viscosity is very sensitive to temperature. The liquid metal at a temperature just above its melting point has a high viscosity. A small

decrease in temperature will also result in its solidification and the process becomes solid-state sintering, which requires a prolonged period for establishing full bonding between the Al particles. The sintering temperature should therefore be above the melting point with a clear margin. If the sintering temperature is excessively high, however, some molten Al near the surface of the compact often oozes out from the compact to form globules. The formation of the globules is due to the tendency of separation of molten Al from the NaCl particles, driven by the poor wetting between them, and is facilitated by the low viscosity. This results in non-uniform distribution of cell size and density in the foam as well as undesired shape distortion. The optimum sintering temperature falls within a narrow range of 670–680 °C for manufacturing pure Al foams. In this temperature range, the molten Al has a fluidity high enough to flow through the disrupted surface and to penetrate the nearby interstices between the particles but not sufficient to separate from the compact.

The shrinkage of the compact during sintering has some influence on the structure of the resultant foam, especially porosity. The foam porosity was 2–4% higher than the initial volume percentage of NaCl. The difference was a result of the joint effect of green porosity and shrinkage. If no shrinkage were present, the difference would have been the green porosity, which varied approximately from 10 to 6% at a compaction pressure of 250 MPa when the volume percentage of NaCl varied from 60 to 80%. The measured increases in the foam porosity, however, were 4–6% lower than the corresponding green porosities. Given the fact that Al is in the liquid form during sintering, there must have been significant shrinkage of the Al matrix in the Al/NaCl compacts. It is understandable that the shrinkage contribution decreased with increasing NaCl volume percentage, because the corresponding Al volume percentage decreased.

4.3. Effects of Sn and Mg

Unlike in solid-state sintering, adding elemental Mg powder to the compacts seems ineffective in the present processing conditions. In solid-state sintering, effective bonding between the Al particles requires sustained intimate contact between the fresh metal surfaces because the process relies on the diffusion of atoms across the interfaces. Since there is always a small amount of air trapped in the compact as voids, these metal–metal interfaces can be easily oxidised when the compact is exposed to the sintering temperature for a prolonged period. Mg added to the compact can absorb the trapped air because of the high reactivity of Mg. The contacts between the Al particles, at which the oxide films have been ruptured during compaction would remain intact during sintering without further oxidation. Mg can also reduce the oxide films at the surface of the Al particles [9,10]. In liquid-state sintering, however, the particles in direct metal contact are largely fused together instantly when the metal is melted. As the metal–metal interfaces disappear immediately, oxidation is unlikely to pose a significant problem,

and the contribution of Mg to the reduction of the oxide film may be small in liquid sintering. Since the proportion of Mg in the compact is very small and the Mg particles are sparsely distributed, the short sintering time may not be sufficient for the Mg to diffuse for long distance to reach the oxide except in its nearest vicinity. The current investigations suggest that Mg addition alone does not result in major benefits to liquid-state sintering in SDP.

Adding relatively small amounts of Sn and Mg together to the powder mixture before compaction and sintering in SDP can, however, have a significant beneficial effect on the quality of the resultant foam. The matrix of the as-produced foam is much denser with a significantly reduced number of voids, as shown in Fig. 8b and d. The improvement is mainly due to the existence of a low viscosity wetting liquid phase. The viscosity of a liquid metal has an Arrhenius dependence on temperature and thus decreases exponentially with temperature above its melting point [12]. Since Sn has a very low melting point (232 °C), its viscosity at the sintering temperature (670–680 °C) is low. In spite of this, a Sn particle in the Al/NaCl compact may still remain in the original location as a droplet instead of spreading out, after being melted, because the liquid Sn does not fully wet the Al particles [5]. In the presence of Mg, however, the wetting angle between the liquid Sn and the Al particles decreases [5]. These low viscosity and wetting liquid Sn droplets can penetrate the fine voids and interstices between the Al particles due to the capillary action and thus increase shrinkage and promote densification. The effect of the densification of the matrix on the physical, chemical and mechanical properties of the as-manufactured Al foam is yet to be investigated.

4.4. Characteristics of the SDP Al foams

For an open-celled Al foam, the structure is usually characterised by its cell size and porosity. These two parameters are predominantly controlled by the particle size and volume fraction of the filler material, i.e. the NaCl powder, in SDP. It was found that the cell morphology and size of the final Al foam closely matched those of the NaCl particles, provided a uniform distribution of the particles in the compact was achieved by thorough blending of the two powders. Like the other P/M processes, one of the most pronounced advantages of SDP is its flexibility. The present results and previous work [4,10] have shown that the cell size and porosity of the Al foams made by SDP can be varied in relatively wide ranges, typically from decades to thousands of microns and from 60 to 85%, respectively, which is difficult to achieve by the preform infiltration or the other foam-manufacturing processes.

In contrast to foams made by the preform infiltration process, Al foams made by SDP have microscopically rough cell surfaces and a less dense matrix. A large number of micro pores or interstices are dispersed over the cell walls and form numerous channels between the cells. This unique microstructure suggests, according to the previous studies

[3,16,17], that the Al foams made by SDP may have lower mechanical properties but much improved damping and energy absorption capacity.

5. Conclusions

The effects of the compaction and liquid-state sintering conditions in SDP on the structure of the resultant Al foams have been studied. The cell morphology and size of the final Al foam closely match those of the NaCl particles. The porosity of the foam is the sum of the initial volume percentage of NaCl and the porosity of the green compact less the shrinkage during sintering. The green porosity decreases with increasing compaction pressure and NaCl/Al ratio. The foam porosity is 2–4% higher than the initial volume percentage of NaCl. The microstructure of the Al matrix is characterised by an interconnected metallic framework with the presence of considerable discontinuous interstices and fine voids as well as primitive particle boundaries in the cell walls. The bonding between the Al particles is facilitated by the localised fusion of the particles through metal–metal contacts. The optimum range of compaction pressure is 200–250 MPa, which brings about efficient disruption of the oxide films of the Al particles without resulting in undesirable defects in the final Al foam such as spalling and cracking. The optimum range of sintering temperature is 670–680 °C, which leads to satisfactory bonding without causing notable Al to ooze out of the compact. Adding elemental Mg powder to the compacts has little effect on liquid-state sintering. Adding elemental Sn together with Mg powders creates a densified Al matrix.

Acknowledgements

We would like to thank Dr. D. Sun, Dr. P. Beahan, Dr. J. Xie, Mrs. M. Hughes and Mrs. A. Rushton of the Department of Engineering, The University of Liverpool, for their assistance in conducting some of the experiments. Han would like to thank The Leverhulme Trust for a Visiting Fellowship and Fung would like to thank the University of Liverpool Graduates Association (Hong Kong) for a Post-graduate Scholarship.

References

- [1] L.J. Gibson, M.F. Asby, Cellular solids, Cambridge University Press, Cambridge, UK, 1997.
- [2] J. Banhart, Prog. Mater. Sci. 46 (2001) 559–632.
- [3] Z.H. Ma, F.S. Han, J.N. Wei, J.C. Gao, Metall. Mater. Trans. A 32 (2001) 2657–2661.
- [4] Y.Y. Zhao, D.X. Sun, Scripta Mater. 44 (2001) 105–110.
- [5] G.B. Schaffer, T.B. Sercombe, R.N. Lumley, Mater. Chem. Phys. 67 (2001) 85–91.
- [6] G. O'Donnell, L. Looney, Mater. Sci. Eng. A 303 (2001) 292–301.

- [7] J. Zhou, J. Duszczyk, *J. Mater. Sci.* 34 (1999) 545–550.
- [8] A. Kimura, M. Shibata, *Appl. Phys. Lett.* 70 (1997) 3615–3617.
- [9] R.N. Lumley, T.B. Sercombe, G.B. Schaffer, *Metall. Mater. Trans. A* 30 (1999) 457–463.
- [10] D.X. Sun, Y.Y. Zhao, *Metall. Mater. Trans. B* 34 (2003) 69–74.
- [11] W.D. Kingery, *J. Appl. Phys.* 30 (1959) 301–306.
- [12] W.D. Kingery, M.D. Narasimhan, *J. Appl. Phys.* 30 (1959) 307–310.
- [13] R.M. German, *Sintering Theory and Practice*, Wiley-Interscience Publication, New York, 1996.
- [14] P. Lu, X. Xu, W. Yi, R.M. German, *Mater. Sci. Eng. A* 318 (2001) 111–121.
- [15] A.C.F. Cocks, *Prog. Mater. Sci.* 46 (2001) 201–229.
- [16] F. Han, Z. Zhu, J. Gao, *Metall. Mater. Trans. A* 29 (1998) 2497–2502.
- [17] F. Han, G. Seiffert, Y. Zhao, B. Gibbs, *J. Phy. D: Appl. Phys.* 36 (2003) 294–302.